

TECHNICAL REPORT: CVEL-12-036
**Optimization of Shunt Capacitor Filters for Reduction of Common Mode
Current in Motor Drives**

Andrew McDowell and Dr. Todd Hubing

Clemson University

April 9, 2012

Table of Contents

1. Abstract.....	3
2. Introduction.....	3
3. Analysis with Network Analyzer.....	5
4. Implementation in Three Phase Inverter System.....	7
5. Optimization of Capacitor Values	14
6. Conclusion	17
References.....	18



1. Abstract

Methods for reducing common mode (CM) Current through optimization of shunt filter capacitor number and placement are being investigated. As the CM current of PWM motor drives can cause electromagnetic interference (EMI) problems as well as currents in the motor's bearings that reduce their life, CM current reduction is an important consideration in the design of a three-phase inverter in order to reduce the need for costly ferrites. It is known that the mutual inductance between the input and output loops of a shunt capacitor filter limits the filtering performance attainable above the LC self resonance frequency. As such, two filter capacitors each with capacitance C spaced apart can obtain much better filtering performance than a single capacitor with capacitance $2C$ at high frequencies.

This research is investigating whether such a dual capacitor filter configuration can be applied to a PWM inverter driving a motor to improve shunt capacitor filtering performance at high frequencies. Results suggest that the dual capacitor configuration can make a more effective filter than a single capacitor configuration for high frequency harmonics created by the PWM inverter system.

2. Introduction

Common mode (CM) currents flowing on the cables between a power inverter and a motor can cause EMI problems as well as currents in the motor bearings that reduce their life. Thus CM current reduction needs to be considered when designing an inverter system. Figure 2-1 shows an example system with a power inverter driving a three-phase brushless motor with a PWM driving scheme. In this system, the CM current flowing on the three phase wires is primarily a result of the changing CM voltage caused by the imbalanced driving scheme driving the parasitic capacitances of the motor windings to the motor case. These parasitic capacitances have relatively large impedances at typical PWM switching frequencies but have relatively small impedances at the higher harmonics created by the fast switching times of the inverter. Thus significant high frequency CM currents flow out on the three phase wires and return on the chassis.

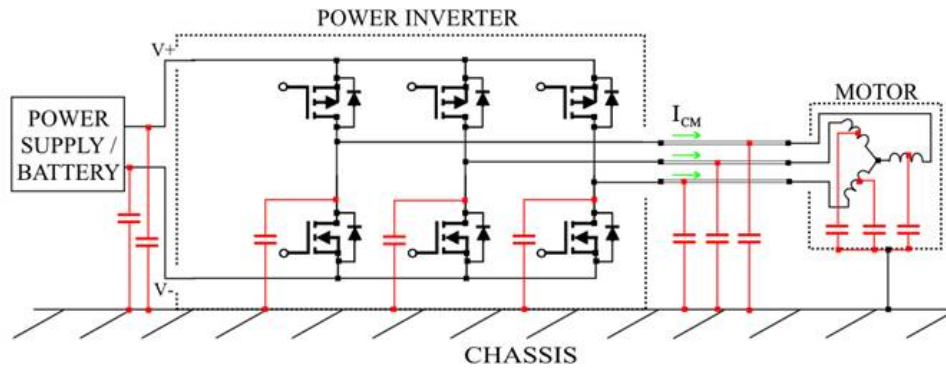


Fig. 2-1. Simplified schematic of motor system with parasitic capacitances shown in red.

Options for reducing this CM current include modified drive schemes, modified physical layout, passive filters, and active filters. Simple shunt capacitor filters are one inexpensive option for reducing the high frequency CM current of three phase PWM motor drives. Though shunt capacitors do not directly filter CM current as do CM chokes and ferrites, they indirectly reduce CM current through reduction of high frequency harmonics that are converted into CM current. At frequencies above the self resonance frequency of the shunt capacitor, however, the mutual inductance between the input and output loops of the capacitor connection to the return path limits the attenuation obtainable [1]. A paper by Zeeff et al. [2] showed that significantly better performance at these high frequencies can be obtained by using two capacitors each of half the original capacitance spaced apart from each other so that the mutual inductance between the input and output loops is minimized. Zeeff's paper used simulations and experiments with a network analyzer to demonstrate that in a 50Ω system, the dual capacitor filter performed significantly better at higher frequencies than a single capacitor with the total capacitance staying constant between the cases. This research is an extension of Zeeff's work that is investigating whether a dual capacitor filter configuration can be applied to a three phase PWM motor system to reduce high frequency CM current as compared to a single capacitor with the same total capacitance.

3. Analysis with Network Analyzer

The PCB shown in figure 3-1 was milled on a 0.0625 inch thick FR4 substrate with double sided 1 oz copper.

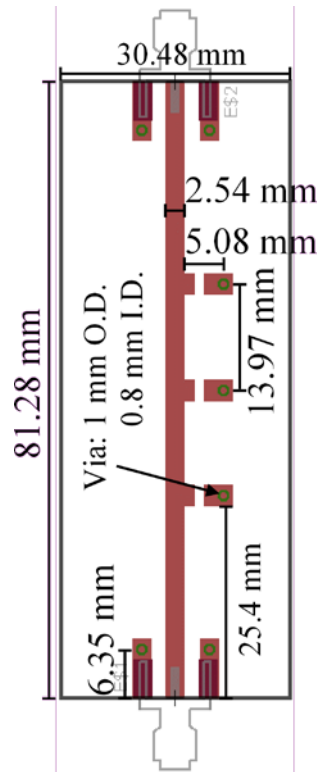


Fig. 3-1. PCB layout of board used to test filter configurations.

Two boards were assembled as shown in figure 3-2. The top board in this figure has two 4.7 nF, 5% tolerance 1206 NPO ceramic capacitors spaced 27.94 mm apart while the bottom board has one 10 nF capacitor of the same type. These values of capacitance were chosen because they are the same values used in Zeff's paper and they can create a self resonance frequency in the range of the CM current spectrum produced by a PWM inverter.

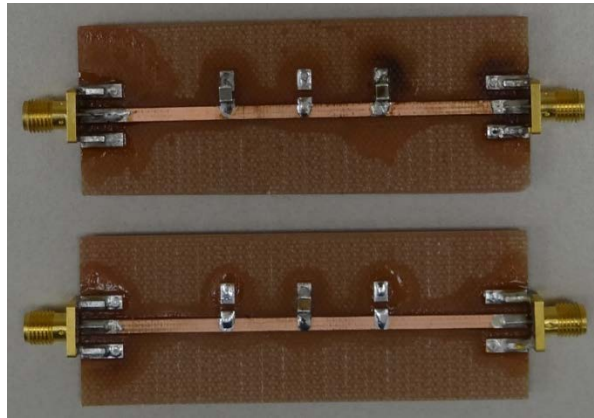


Fig. 3-2. Constructed boards used to test dual and single capacitor filter configurations.

The boards were tested with a Hewlett Packard 87533ES Network analyzer from 1 MHz to 500 MHz. The measured insertion losses (S_{21}) for the two different configurations are shown in figure 3-3. Note that at frequencies above 40 MHz, the dual capacitor filter has significantly greater insertion loss than the single capacitor filter. However, filtering performance of the dual capacitor filter is considerably worse than the single capacitor at around 18 MHz due to a resonant parallel combination of inductances and capacitances to ground at this frequency. If the parasitic inductance connections of the capacitors were made smaller as is recommended for shunt capacitor filters, the self resonant frequency would increase, so the improvements due to the dual capacitor filter would not occur until higher frequencies.

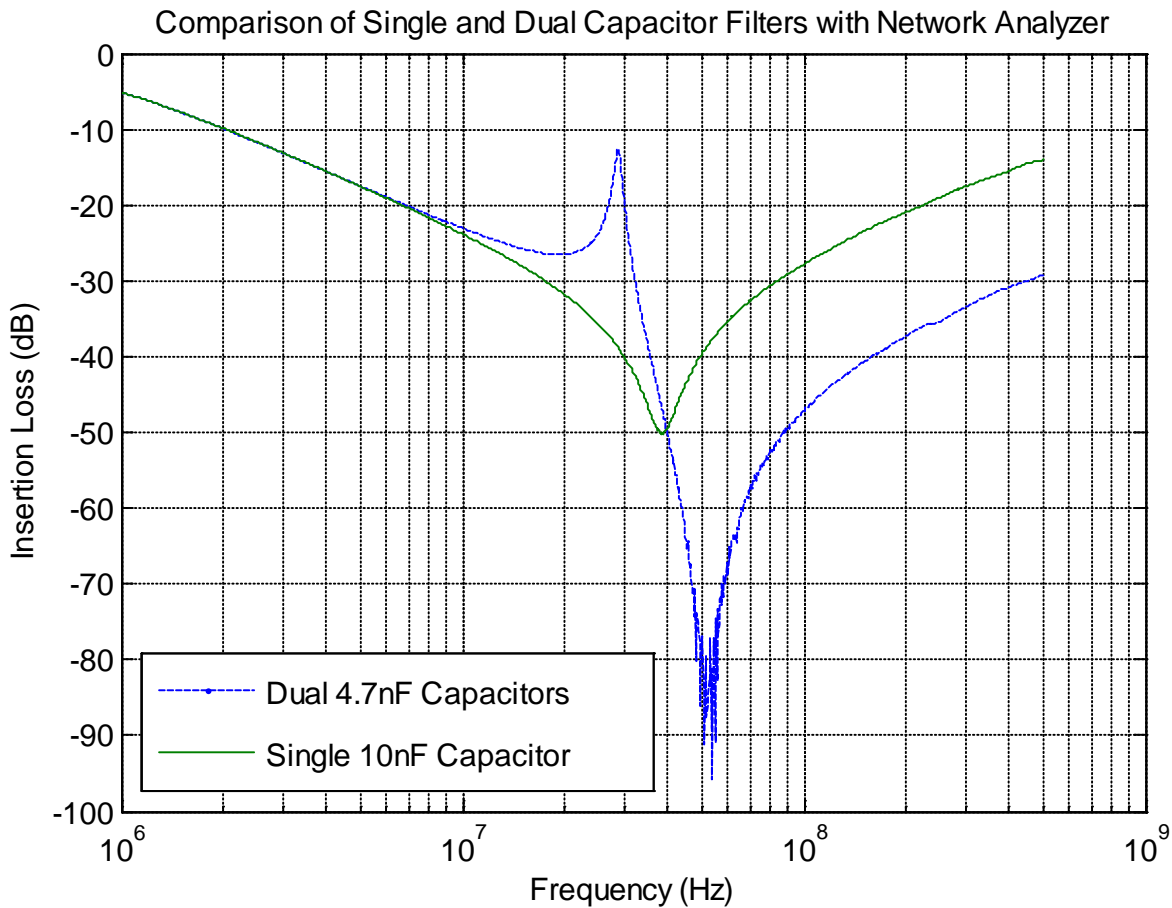


Fig. 3-3. Comparison of single and dual capacitor filters.

4. Implementation in Three Phase Inverter System

Inverter and Motor

A three phase motor and inverter and a CA6 inverter was supplied by John Deere. Note that each phase has a passive filter consisting of a 1 nF capacitor in series with a 49.9 Ω resistor connecting the phase output to heat sink that was removed prior to this experiment. The output capacitance per phase was about 4.3 nF as measured with a BK Precision 878 universal LCR meter after removal of these filters. The inverter is powered by a BK Precision high current regulated power supply set to 48 VDC. The heat sink is electrically connected to a metal sheet which also makes contact with the case of the motor. This electrical node which is henceforth called 'chassis' is isolated at DC from the supply rails

of the inverter. However, about 6.1 nF of capacitance was measured between the chassis and either the positive or negative supply rail.

Extension Board

An extension board for testing filter configurations was designed and milled on a 0.0625 inch thick FR4 substrate with double sided 2 oz copper. Figure 4-1 shows the layout and dimensions of this board. The three pads on each of the three traces are for connecting the 5% tolerance 1206 NPO ceramic capacitors. Like in the network analyzer tests from section 3, when dual 4.7 nF capacitors were tested, the outer two pads were used, while when a single 10 nF capacitor was tested, the center pad was used.

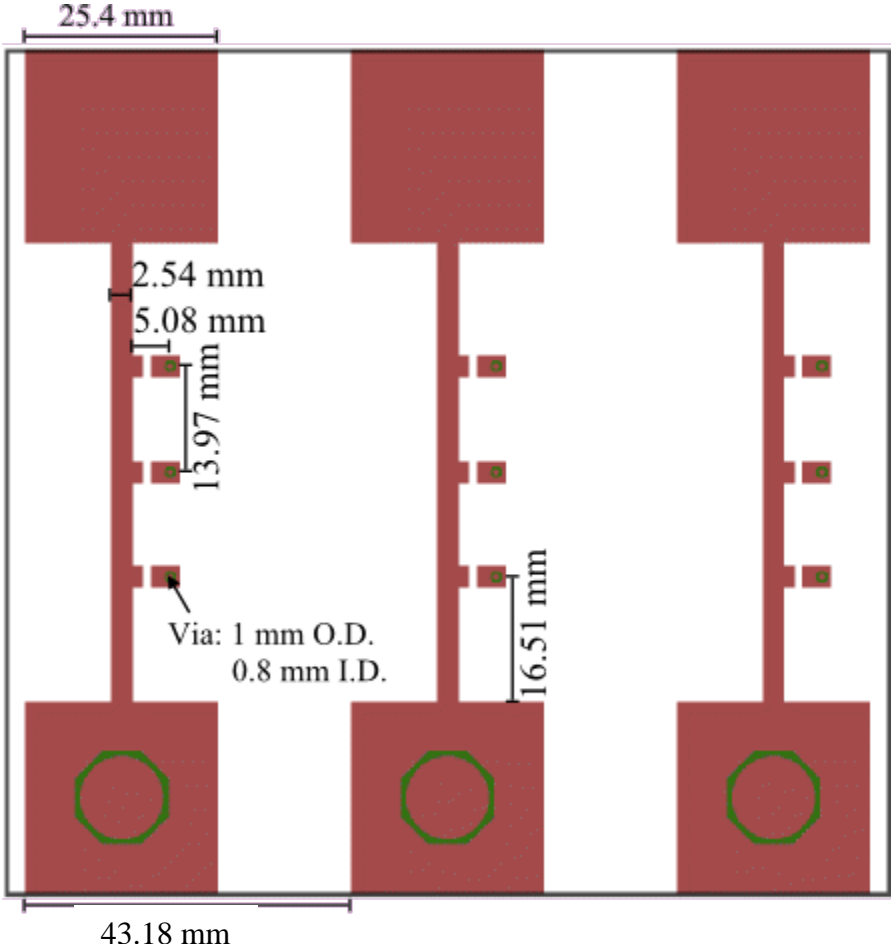


Fig. 4-1. Layout of board for testing filters with inverter.

In order to support the high currents required by the motor, a 1.6 mm diameter copper wire was soldered to the traces and all the high current pads were coated with solder about 2 mm thick. The experimental setup with the completed extension board is shown in figure 4-2.

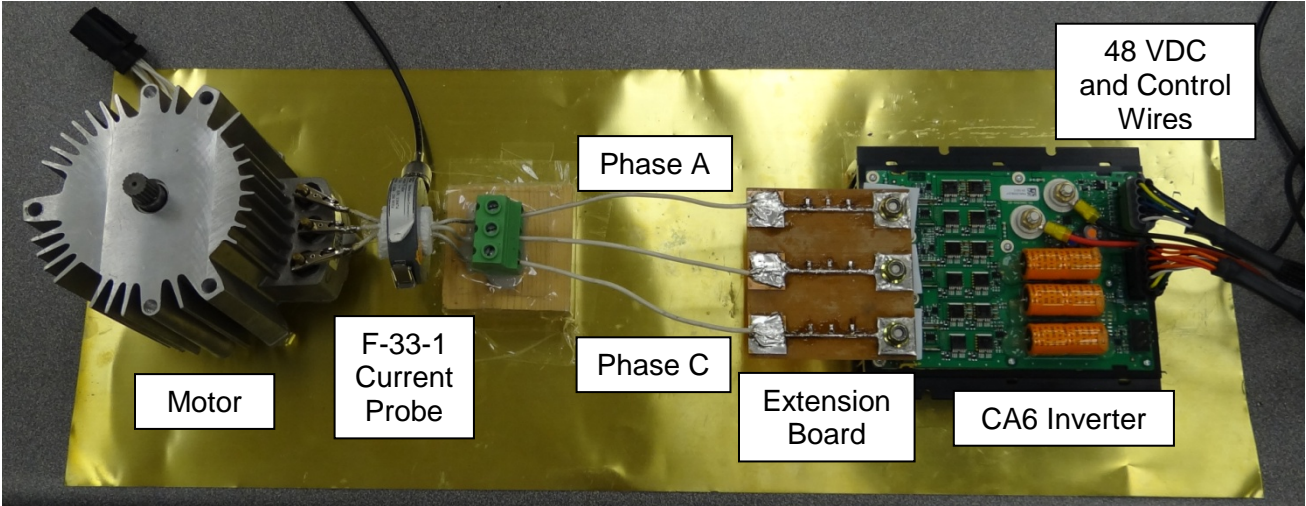


Fig. 4-2. Photo of test setup with 40 cm cable length.

The bottom of the extension board is a solid ground plane. The connection between the main test setup chassis and the bottom of the extension board is made with 3M #1181 conductive copper tape as shown in figure 4-3.

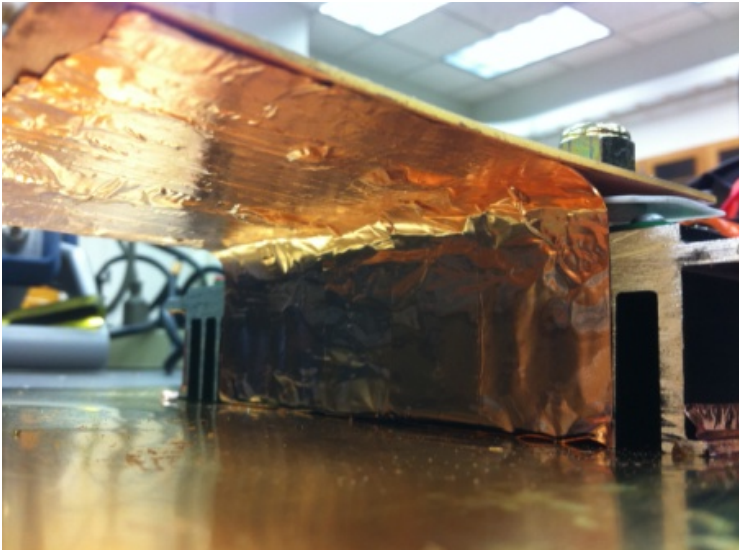


Fig. 4-3. Conductive copper tape used to connect chassis to bottom of extension board.

The experiment was also done with a longer cable length of about 170 cm. Note that in both setups the wires are approximately 7 cm above the chassis metal sheet in the path from the inverter to the motor.

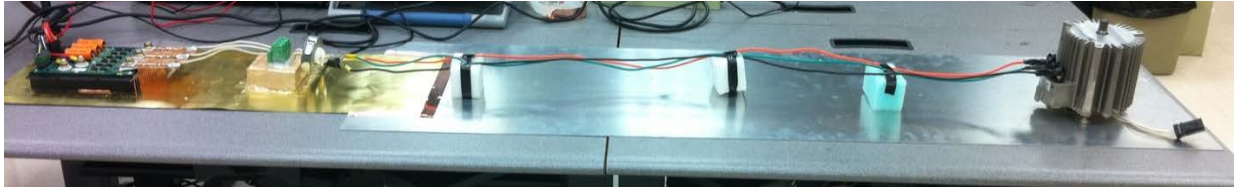


Fig. 4-4. Photo of test setup with 170 cm cable length.

Test procedure

A BK Precision high current regulated power supply powered the experimental setup with 48 VDC. The control box was adjusted to select the ABC: 100 space vector, and the duty cycle was adjusted so that the average current on phase A was 50 A as measured by a TPO 150 current probe clamped around phase A and connected to a Tektronix MSO 4104 oscilloscope. The CM current was measured using a Fischer Custom Communications F-33-1 current probe connected to a Rohde and Schwarz FSL Spectrum analyzer. The RBW of the spectrum analyzer was set to 3 kHz, the VBW was set to 10 kHz, the attenuation was set to 20 dB, the reference level was set to 0 dBm, and the frequency range was set to 0 Hz – 100 MHz. With these settings, the sweep time was automatically set to 11 s. This frequency range was selected because measurements with a larger frequency range showed that there were no significant harmonics in the CM current at higher frequencies.

The transfer impedance of the F-33-1 current probe is 5 Ω from 1 MHz to 250 MHz. Thus the CM current, in Amperes, flowing in the three phase wires can be determined from the dBm values measured on the spectrum analyzer, m , by:

$$I_{CM} = \sqrt{0.002 \times 10^{m/10}}. \quad (1)$$

Thus for example, a measurement of -20 dBm corresponds to about 4.5 mA of CM current.

Results

Figure 4-5 shows the raw data for the 40 cm motor cable configuration. The noise floor is the CM current measured with the inverter powered off.

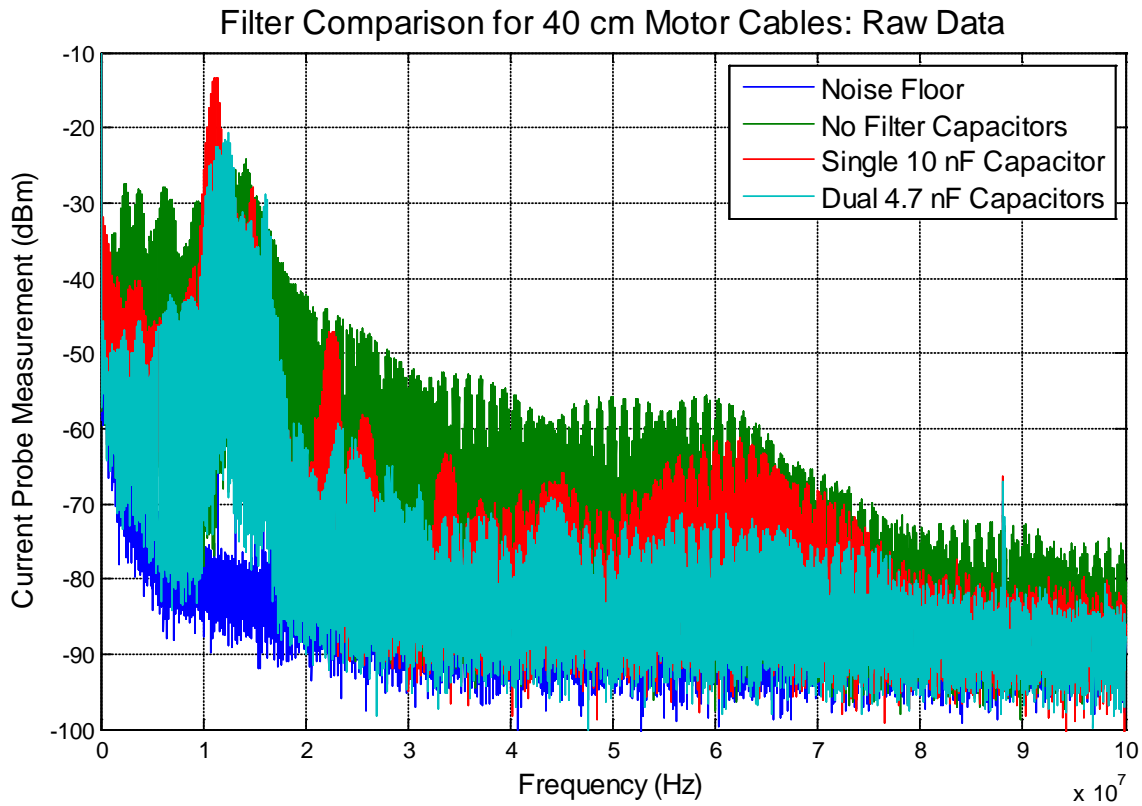


Fig. 4-5. Raw data for 40 cm motor cable configuration.

As the data exhibit considerable variation and we are only interested in the maximal components of the data, a method of smoothing data while preserving maxima was performed. Each of the data sets underwent four iterations of linear interpolation between all local maxima yielding the smoothed plots shown in figure 4-6.

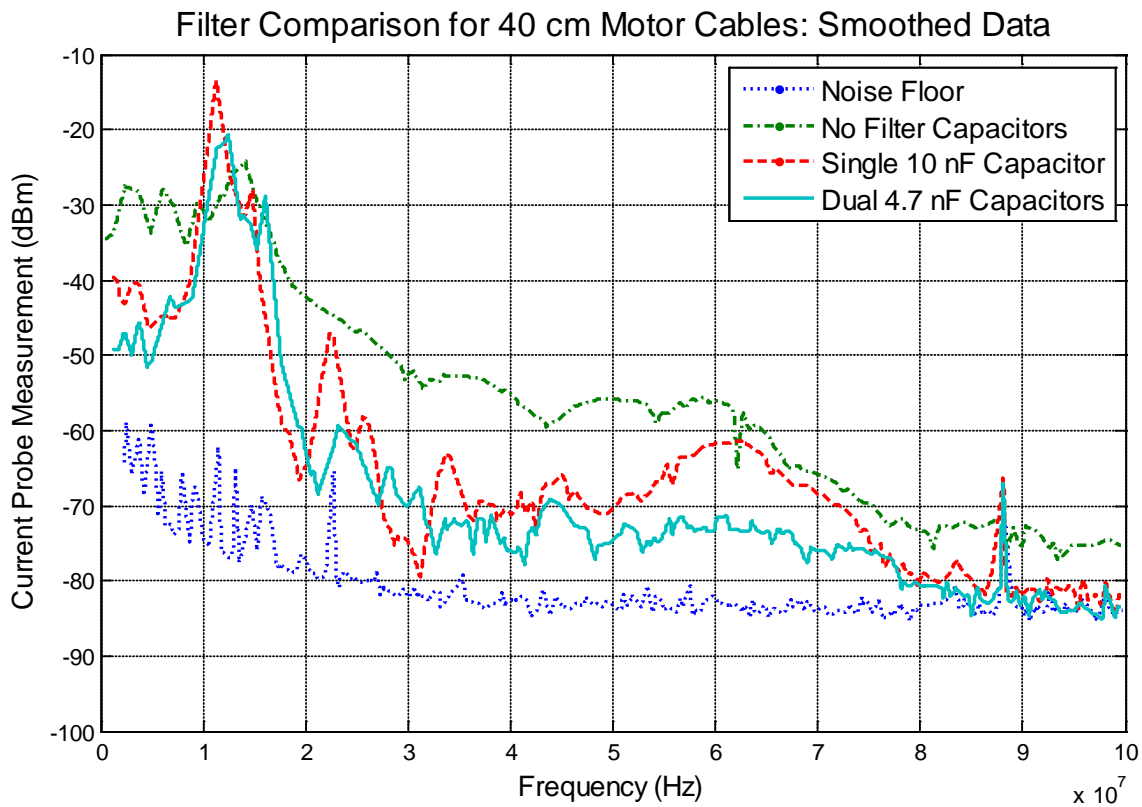


Fig. 4-6. Smoothed data for 40 cm motor cable configuration.

For the 40 cm case, both filter configurations generally reduce CM current above around 20 MHz as compared with the unfiltered output. The dual capacitor configuration is more effective in filtering CM current above about 40 MHz. This result is consistent with the results obtained with the network analyzer. It is suspected that the increased CM current with both filter configurations around 12 MHz is due to a resonance similar to the one causing the 18 MHz peak observed in section 3.

Similar plots for the 170 cm motor cable configuration are shown in figures 4-7 and 4-8 below.

Filter Comparison for 170 cm Motor Cables: Raw Data

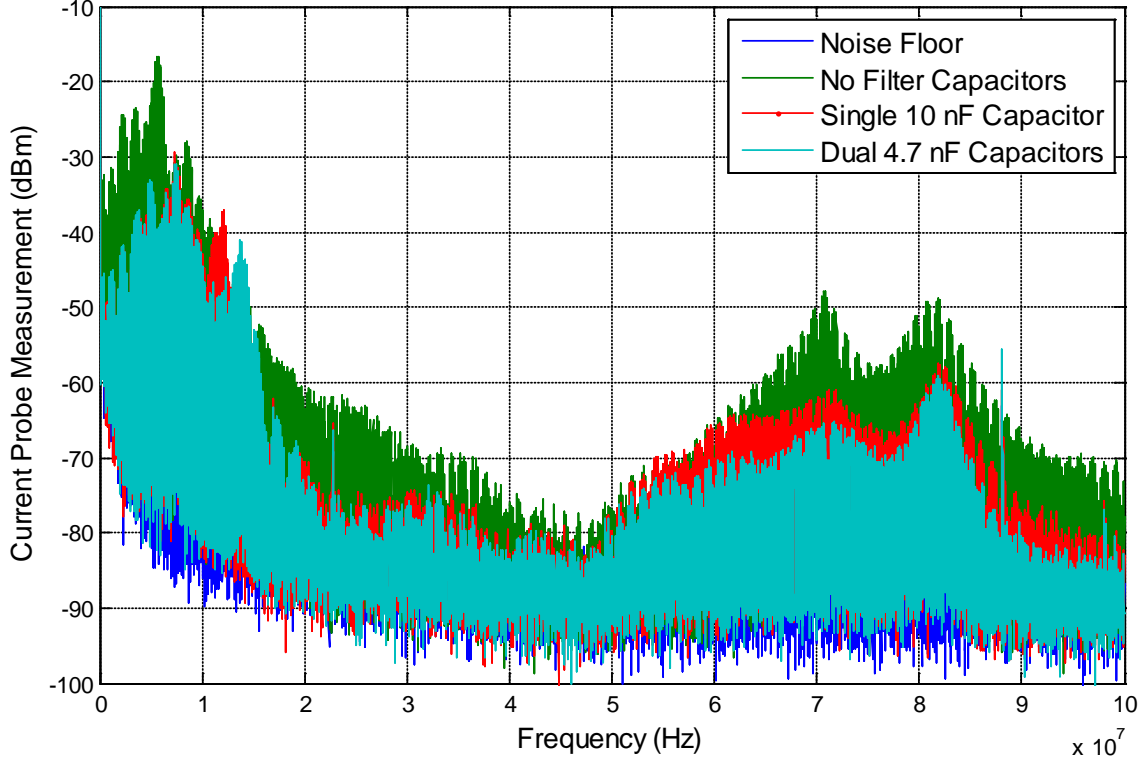


Fig. 4-7. Raw data for 170 cm motor cable configuration.

Filter Comparison for 170 cm Motor Cables: Smoothed Data

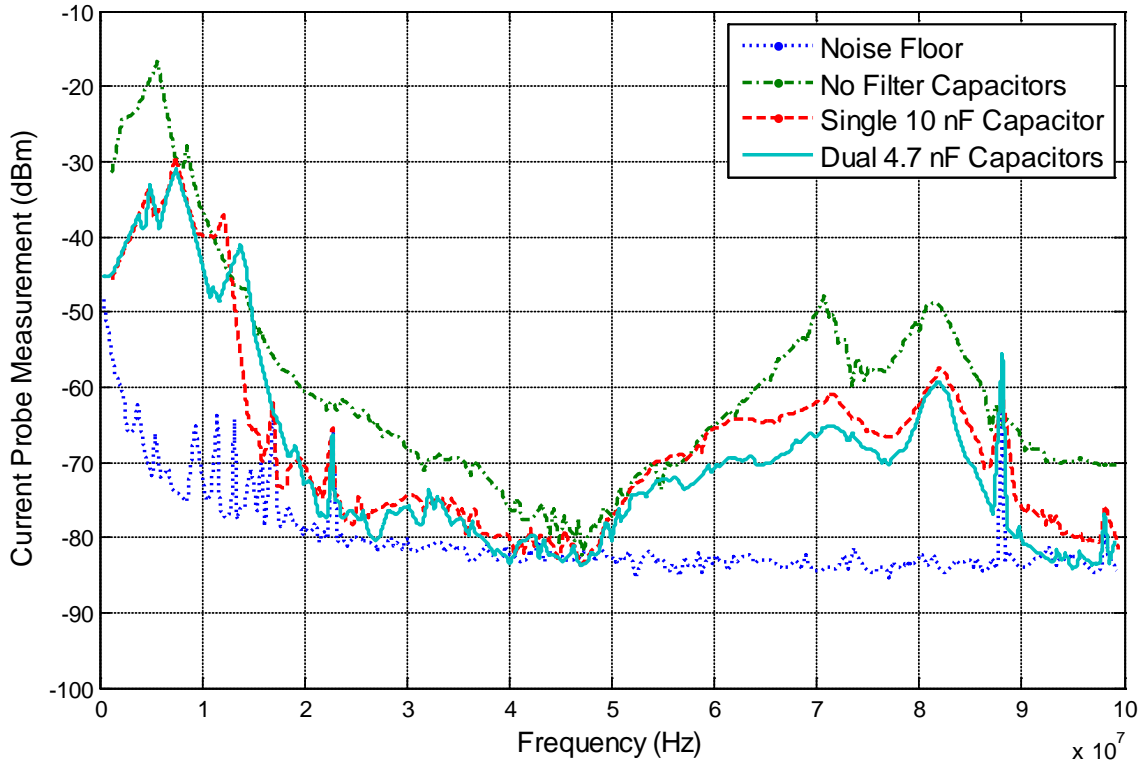


Fig. 4-8. Smoothed data for 170 cm motor cable configuration.

Note that for the 170 cm case both filters reduce the CM current at most frequencies including the peak frequency as compared with the unfiltered output. The dual capacitor filter again performs better at higher frequencies than the single capacitor filter. Because there were certain frequencies where the CM current of the unfiltered output was lower than that of the filtered output, more experimentation was done by testing additional filter configurations with a network analyzer.

5. Optimization of Capacitor Values

Seven identical boards were milled with the layout shown in figure 5-1 on a 0.0625 inch thick FR4 substrate with double sided 1 oz copper. Note that there are two 0805 components in series connecting each of the two vias to the main 50 Ω trace. This configuration was chosen to allow testing resistors in series with the filter capacitors to potentially damp resonant peaks in the insertion loss. For all cases, the capacitors were placed closest to the traces and the smaller capacitance for asymmetric cases was placed closest to port 2 of the network analyzer. In the cases without series resistance, a 0 Ω 0805 resistor was used.

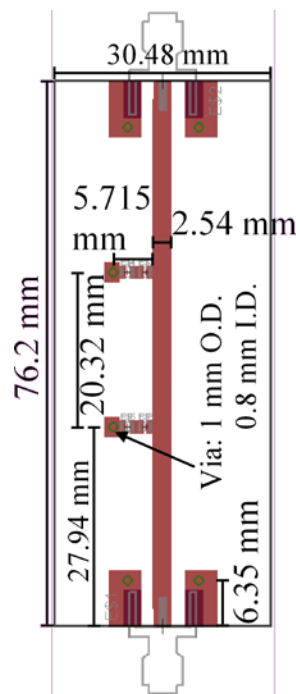


Fig. 5-1 Board layout used for tests in section 5.

The assembled boards with the different filter configurations marked are shown in figure 5-2.

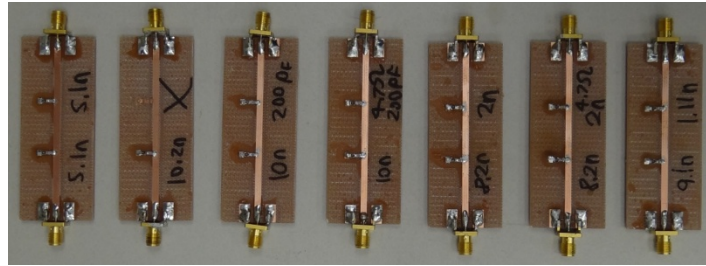


Fig. 5-2 Boards constructed for tests in section 5.

Different values for the capacitors were tried on the boards tested with a network analyzer in an attempt to provide more effective filtering across all frequencies. Note that the boards used in these tests were different from the boards tested with the network analyzer in section 3 so the self resonance frequencies differ. All capacitances were implemented with a single 0805 NPO ceramic capacitor except for the 10.2 nF and 1.11 nF cases. The 10.2 nF capacitance was obtained by placing a 200 pF capacitor on top of a 10 nF capacitor in a parallel combination, while the 1.11 nF capacitance was obtained by placing a 200 pF capacitor on top of a 910 pF capacitor in a parallel combination. Figures 5-3 and 5-4 show the results of this experiment. Note that of the configurations tested, the combinations of 8.2 nF and 2 nF or 8.2 nF and 2 nF in series with 4.7 Ω provided what may be the best filtering across the frequencies tested.

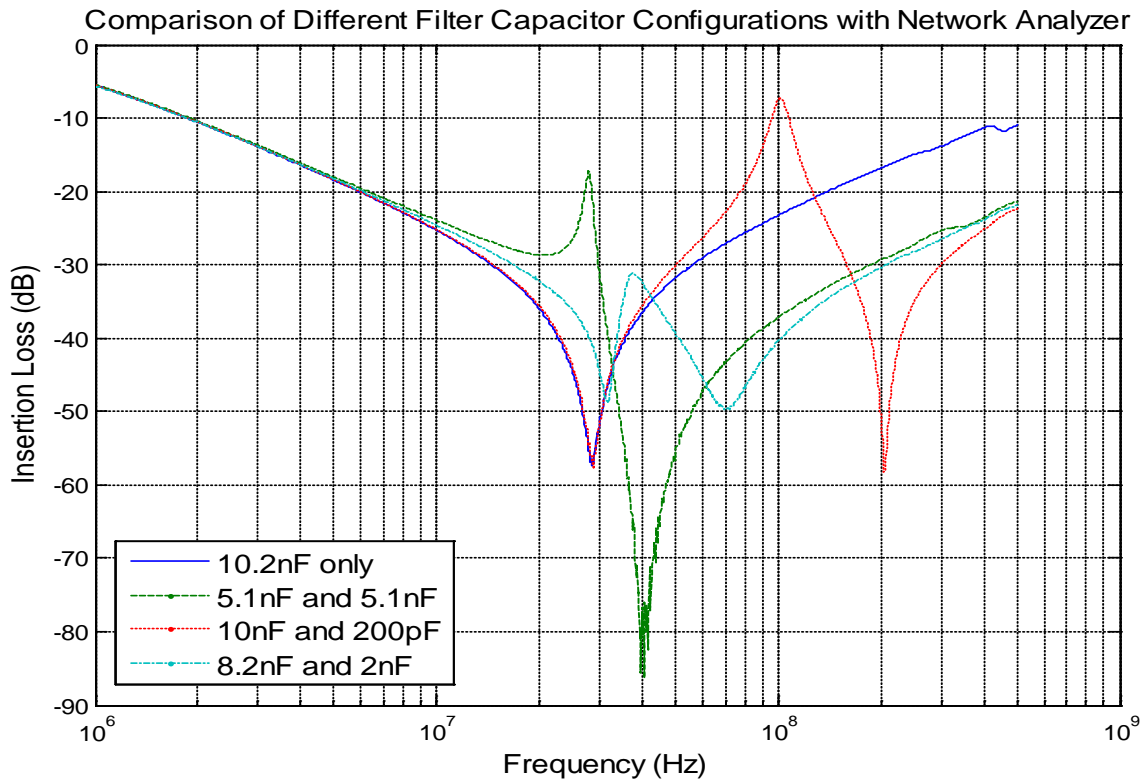


Fig. 5-3. Insertion losses of various filter configurations, each with 10.2 nF total capacitance.

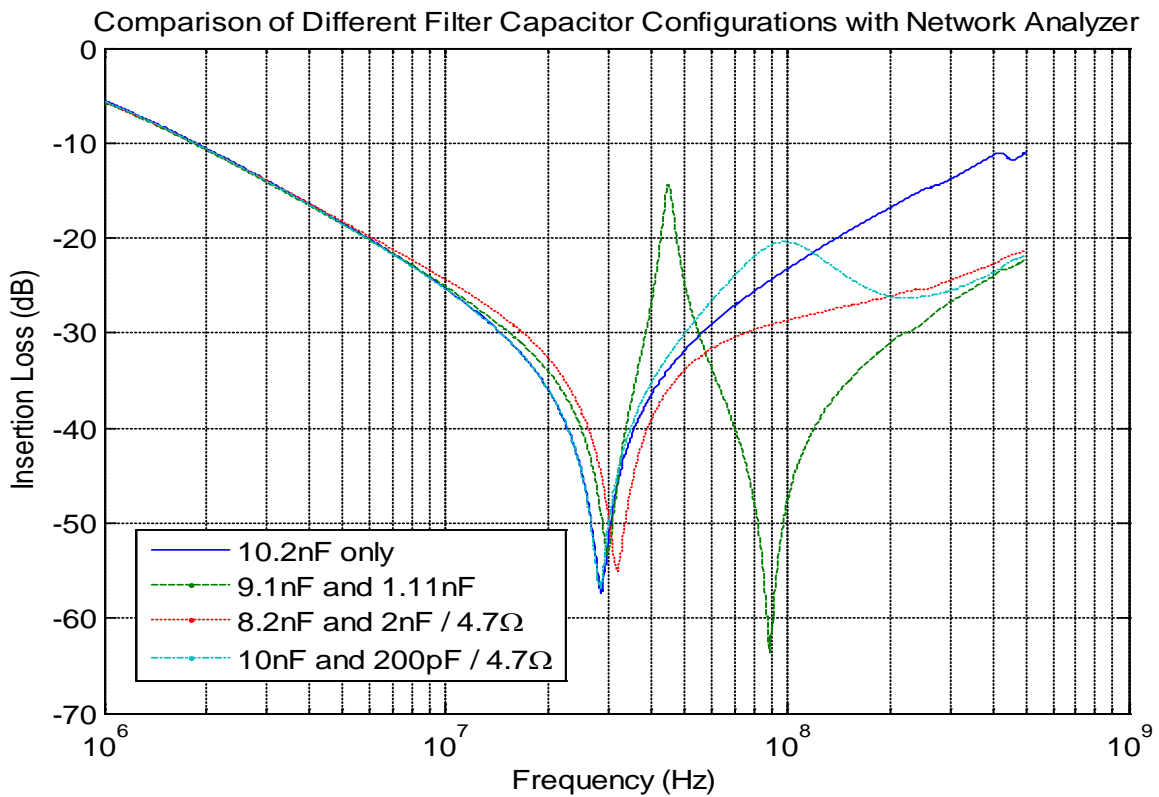


Fig. 5-4. Insertion losses of other filter configurations with 10.2 nF total capacitance including two configurations with series 4.7 Ω resistance on side with less capacitance.

An asymmetric dual capacitor configuration similar to the 8.2 nF and 2 nF capacitor case tested with the network analyzer was tested on the extension board to see if the promising results with the network analyzer can successfully be extended to a practical inverter system. The results for this investigation are shown in figure 5-5 below. A 1.8 nF capacitor was used instead of the 2 nF capacitor used in the network analyzer experiment in order to keep the capacitance no greater than the single 10 nF capacitor case. The 8.2 nF capacitor was mounted on the pads closer to the inverter and the 1.8 nF capacitor was mounted on the pads closer to the motor. The asymmetric dual capacitor configuration appears to have similar filtering performance than the symmetric dual capacitor case.

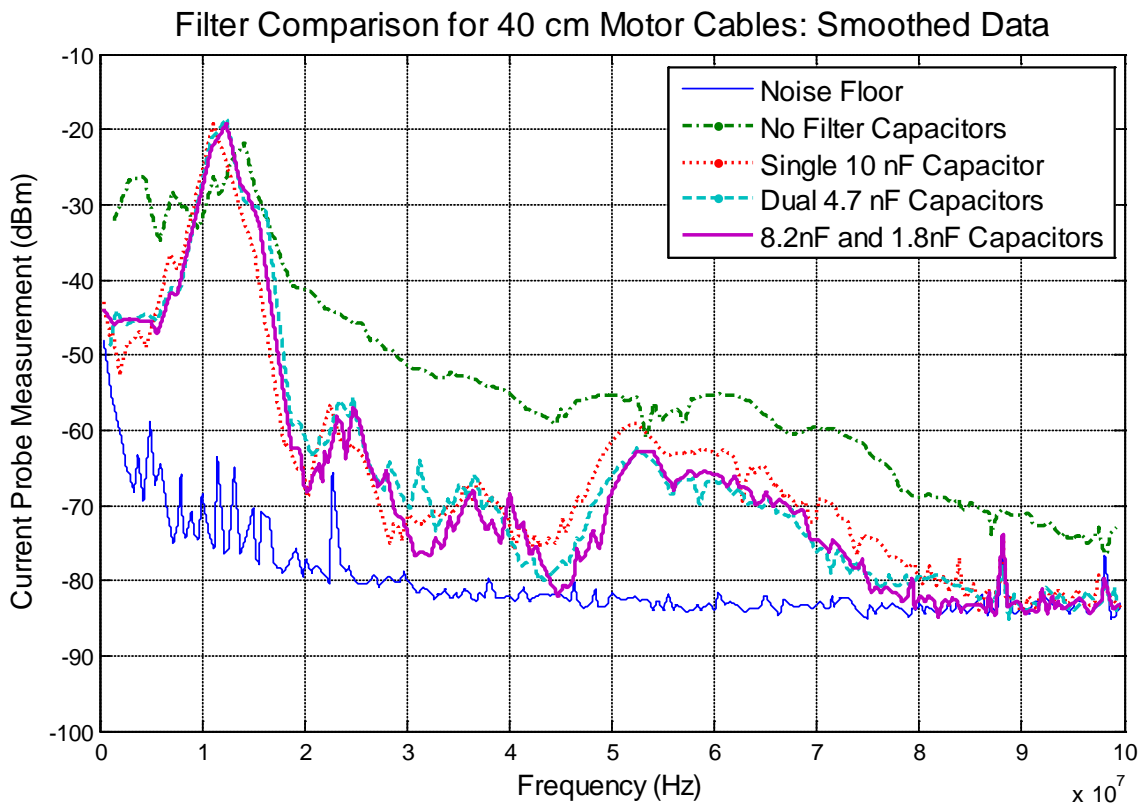


Fig. 5-5. Additional filter configuration tested with motor inverter system.

6. Conclusion

A simple and inexpensive way to improve the performance of a filter capacitor above its self resonant frequency is to replace the capacitor with two smaller capacitors separated from each other. Though the effectiveness has been demonstrated in filtering the CM current of a power inverter at high

frequencies, optimizing the performance across all frequencies is currently being investigated. Ongoing research is working on understanding the problem better so that methods for optimization of shunt capacitor filters specific to reduction of CM current in motor inverter systems can be well formulated. In particular, future work will attempt to better understand and solve the problem that either filter configuration increases CM current relative to the unfiltered output at certain frequencies.

References

- [1] Olsen, C.N.; Van Doren, T.P.; Hubing, T.H.; Drewniak, J.L.; DuBroff, R.E.; , "Improving the high-frequency attenuation of shunt capacitor, low-pass filters," *Electromagnetic Compatibility, 2001. EMC. 2001 IEEE International Symposium on* , vol.1, no., pp.487-489 vol.1, 2001.
- [2] Zeeff, T.M.; Hubing, T.H.; Van Doren, T.P.; Pommerenke, D.; , "Analysis of simple two-capacitor low-pass filters," *Electromagnetic Compatibility, IEEE Transactions on* , vol.45, no.4, pp. 595- 601, Nov. 2003.